JOURNAL OF MAGNETIC RESONANCE **124,** 165–171 (1997)
ARTICLE NO. MN961023

Far-Off-Resonance Averaging of Dipolar Interactions in Solids

I. CHANG, G. DIEZEMANN, G. HINZE, R. BÖHMER, AND H. SILLESCU

Institut für Physikalische Chemie, Johannes Gutenberg-Universität, Mainz, D-55099 Mainz, Germany

Received July 29, 1996; revised October 2, 1996

The far-off-resonance performance of several line-narrowing sequences is investigated. Both theoretically and experimentally, it is found that transverse relaxation times, dominated by dipole–dipole interactions, are most effectively prolonged not only on-resonance but also for certain, generally large, resonance offsets. These correspond to a situation when, during the basic pulse separation, the frequency offset rotates the toggling-frame Hamiltonian by multiples of 180°. The implications of these results for the study of macroscopic translational diffusion using static-field-gradient NMR are discussed. © 1997 Academic Press

INTRODUCTION

Since the discovery of the Hahn echo, NMR in inhomogeneous fields has been used to study translational motion in liquids. Slow molecular transport, as manifested in the mass diffusion in solids, is also accessible via NMR relaxation techniques (*1*), if additional information, e.g., on microscopic jump lengths, is available. In the case of incommensurably ordered crystals, information about the modulation wave vectors is used to deduce diffusion coefficients (*2*). For the determination of very small *macroscopic* diffusion coefficients, large external magnetic-field gradients are required (*3, 4*). Using two vastly different approaches, viz. an anti-Helmholtz arrangement of superconducting solenoids (*5*) or the inhomogeneous field distribution in the vicinity of a wire driven by large current pulses (*6*), field gradients on the order of $g = 100$ T/m and more have been achieved. However, the spatial resolution of gradient NMR methods is limited not only by the magnitude of the available gradient strength, but also by the evolution time τ during which the transverse magnetization is subjected to this gradient. This restriction is particularly severe in studies of solids, where the nuclear dipole–dipole interactions cause a dephasing of the transverse magnetization on the time scale of relatively short spin–spin relaxation times T_2 on the order of 100 μs or less.

It is possible to mitigate the rapid dephasing of transverse magnetization by the application of multiple-pulse irradiation. The most commonly used multiple-pulse sequences are based on the four-pulse WAHUHA (*7*) or the eight-pulse MREV (*8*) cycles. Although the MREV cycle is relatively robust against various pulse imperfections, multiple-pulse sequences are usually considered to require carefully adjusted spectrometers.

Recently it has been shown that the MREV sequence can also be used in strongly inhomogeneous magnetic fields to yield an up to 20-fold prolongation of the effective T_2 (*9*). This observation, which then allowed diffusion studies to be carried out well in the solid state, is quite remarkable, if one recalls that the Larmor frequency variation across the excited sample volume is on the order of 1 MHz. Thus, if one attempts to optimize the pulse sequence for one particular slice within the sample, one inevitably must accept nonideal conditions for the rest of the specimen.

The off-resonance performance of multiple-pulse sequences has been studied previously only for relatively small resonance offsets $\Delta\omega$. It has been found that $\Delta\omega/2\pi$ on the order of a few kilohertz can lead to an additional (usually slight) increase of the spectral resolution (*10*). In the framework of an average Hamiltonian treatment, this phenomenon is understood to be an effect of second averaging of those parts of the dipolar interaction which are nonsecular in the frame rotating with the effective off-resonance frequency (*11*). It has even been demonstrated a long time ago that, with a suitably chosen offset frequency, an effective Hamiltonian equivalent to that of the conventional (four-phase) WAHUHA cycle can be produced on spectrometers which can be operated on only two different RF phases (*12*). The off-resonance frequency employed in these previous studies usually did not exceed about 5 kHz.

It is interesting to note that the relevant resonance offsets that we have to deal with in the present experiments are larger by up to two orders of magnitude. Therefore, we first derive the conditions under which the four- and eight-pulse sequences are effective even under certain far-off-resonance conditions. After giving some experimental details, we compare the theoretical expectations concerning the off-resonance dependence of the effective transverse relaxation times with experimental results obtained in homogeneous magnetic fields for various $\Delta\omega$. Experiments in large gradient fields are then presented in order to discuss the optimum conditions for the performance of diffusion measurements. We then conclude with a summary of our findings.

1090-7807/97 $25.00

THEORETICAL CONSIDERATIONS

The basic pulse sequences that we have used and analyzed under far-off-resonance conditions are the WAHUHA and the MREV cycles depicted in Fig. 1. Between two pulses, separated by the interval τ_0, the density operator evolves under the action of the time-evolution operator

$$U_z := U_{CS,z}U_{off,z}U_{D,z}. \quad [1]$$

Here

$$U_{off,z} = \exp\{i\Delta\omega I_z\tau_0\}$$

and

$$U_{CS,z} = \exp\{i\sigma I_z\tau_0\} \quad [2]$$

describe the effects of the off-resonance $\Delta\omega$ and of the chemical-shift interactions σ while

$$U_{D,z} = \exp\{-iH_{D,zz}\tau_0\} \quad [3]$$

with the truncated Hamiltonian

$$H_{D,zz} = \frac{1}{2}\sum_{i\neq j} b_{ij}[3I_z^{(i)}I_z^{(j)} - \mathbf{I}\cdot\mathbf{I}] \quad [4]$$

accounts for the dipolar interactions. As usual, $b_{ij} = -\gamma^2\hbar P_2(\cos\theta_{ij})/r_{ij}^3$, with P_2 denoting the second Legendre polynomial and θ_{ij} the angle enclosed by the external magnetic field and the vector connecting two nuclei i and j. For convenience, we will first set $\sigma = 0$ but return to the properties of the chemical-shift interaction at the end of this section.

The propagator of Eq. [1] as seen from the toggling frame reads, for one cycle period t_c of, e.g., the WAHUHA experiment (*13*),

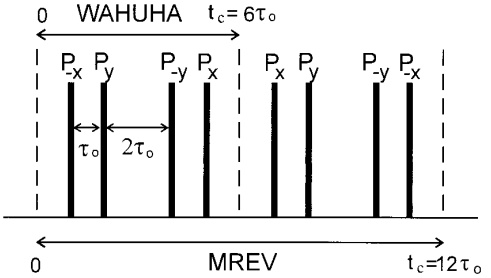

FIG. 1. Schematic representation of the WAHUHA and MREV pulse cycles.

$$U(t_c) = U_zU_yU_xU_xU_yU_z \quad [5]$$

which can be written as

$$U(t_c) = U_D(t_c)U_{off}(t_c). \quad [6]$$

This latter representation has the advantage that the time-evolution operators for the resonance offset and the dipolar interaction can be treated separately. In order to carry out this factorization, one uses Eq. [5] in conjunction with Eq. [1] and repeatedly inserts $U_{off,\alpha}^{-1}U_{off,\alpha}$ with $\alpha = x, y, z$ into the right-hand side of the resulting equation. One then finds

$$U_{off}(t_c) = U_{off,z}U_{off,y}U_{off,x}U_{off,x}U_{off,y}U_{off,z} \quad [7]$$

and

$$U_D(t_c) = U_{D,z}U_{D,y}^{(z)}U_{D,x}^{(yz)}U_{D,y}^{(yz)}U_{D,z}^{(xxyz)}U^{(yxxyz)} \quad [8]$$

with, e.g., $U_{D,x}^{(yz)} = U_{off,z}U_{off,y}U_{D,x}U_{off,y}^{-1}U_{off,z}^{-1}$.

The separation of the time-evolution operators according to Eq. [6] is essential, since $U(t_c)$ is periodic but in general is not cyclic and thus cannot be evaluated in the framework of average Hamiltonian theory. The transformed dipolar interaction and the offset interaction can thus be treated independently. The definition of an average dipolar Hamiltonian associated with $U_D(t_c)$ in Eq. [8] is then meaningful if the cycle time is kept small ($\tau_0 \ll T_2$). As for $U_{off}(t_c)$, no short-time expansion of Eq. [7] is possible for sufficiently large $\Delta\omega$. However, this also is not necessary, since the transformation of the density matrix under the composite rotation expressed by Eq. [7] can be carried out analytically in a straightforward manner and yields

$$I_\alpha(t_c) = U_{off}^{-1}(t_c)I_\alpha(0)U_{off}(t_c) = \sum_{\beta=x,y,z} A_{\alpha\beta}(\tau_0\Delta\omega)I_\beta. \quad [9]$$

An inspection of the coefficients $A_{\alpha\beta}(\tau_0\Delta\omega)$ obtained for the WAHUHA cycle shows that U_{off} is cyclic, i.e., fulfills the condition $I_\alpha(t_c) = I_\alpha(0)$, for $\tau_0\Delta\omega = n\pi/2$ and $n\pi$ with $\alpha = x$ and y, respectively. Here n is an integer number. An analogous calculation for the MREV sequence showed that both I_x and I_y remain invariant under the action of the off-resonance operator for $\tau_0\Delta\omega = n\pi/2$.

Cyclicity of U_{off} is a necessary but not a sufficient prerequisite for the off-resonance averaging to be as effective as averaging under on-resonance conditions. In addition, one must investigate how the dipolar interaction transforms under far-off-resonance conditions. For τ_0 much smaller than the spin–spin relaxation time T_2 the dipolar time-evolution operator, Eq. [8], can be written as usual as

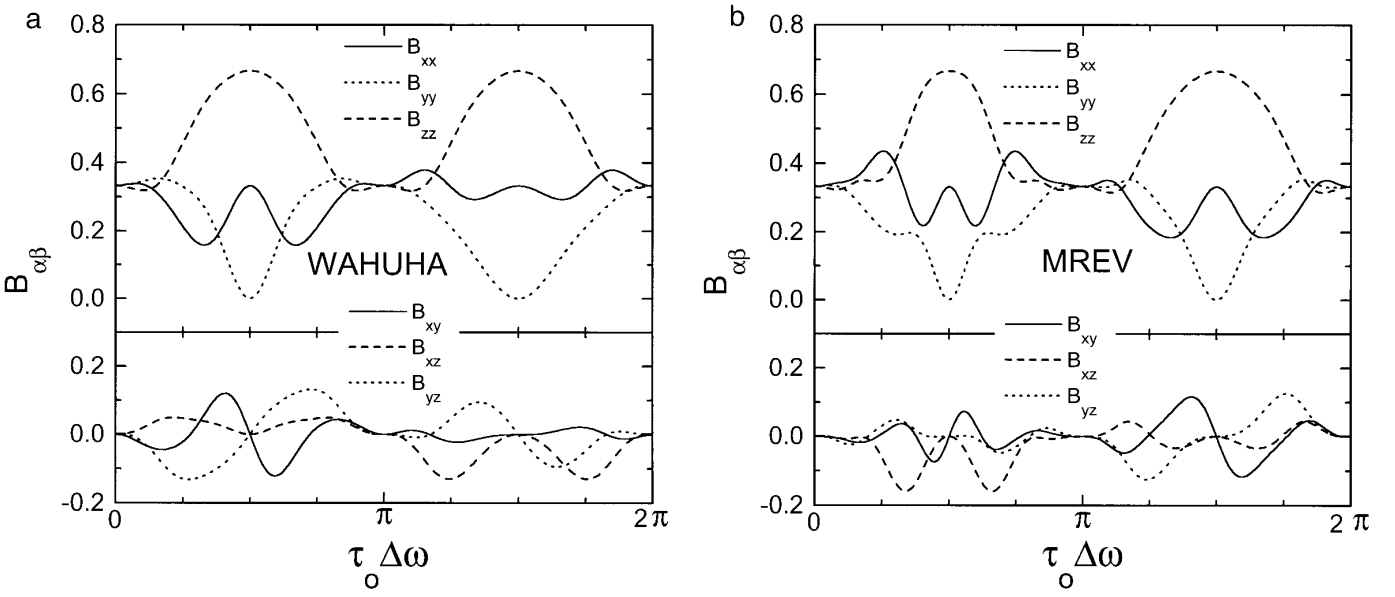

FIG. 2. Coefficients $B_{\alpha\beta}$ for (a) the WAHUHA and (b) the MREV cycles. Note that while the line-narrowing condition is fulfilled at the nodes of the $B_{\alpha\alpha}$ patterns, i.e., at $n\pi$, the coefficients are only periodic with respect to $2n\pi$.

$$U_{\mathrm{D}}(t_{\mathrm{c}}) = \exp\{-i\overline{H_{\mathrm{D}}}t_{\mathrm{c}}\}. \qquad [10]$$

Here the average Hamiltonian

$$\overline{H_{\mathrm{D}}} = \sum_{\alpha\beta} B_{\alpha\beta}H_{\mathrm{D},\alpha\beta} \qquad [11]$$

resulting from Eq. [8] can be considered the first term in the Magnus expansion with, e.g., the operator $H_{\mathrm{D},xy}$ written as defined in Eq. [4], however with $I_z^{(i)}I_z^{(j)}$ replaced by $[I_x^{(i)}I_y^{(j)} + I_y^{(i)}I_x^{(j)}]$. Using Eqs. [8] and [10] the coefficients $B_{\alpha\beta}$ in Eq. [11] were evaluated for the WAHUHA and MREV sequences and are shown in Fig. 2. It is evident that the $B_{\alpha\beta}$ patterns for both sequences exhibit nodes, with the coefficients being $\frac{1}{3}$ for $\alpha = \beta$ and 0 for $\alpha \neq \beta$, at the frequencies given by

$$\tau_0\Delta\omega = n\pi. \qquad [12]$$

Here n denotes an integer number. Thus, for $\Delta\omega$ chosen to satisfy Eq. [12], the effective linewidth under multiple-pulse irradiation is (as for $\Delta\omega = 0$) dominated by those parts of the dipolar interaction that do not commute with the operator defined in Eq. [11]. These contributions give rise to a residual linewidth δ_{res} or correspondingly to a maximum transverse dephasing time T_2^{max}.

For the calculations of the effective spin–spin relaxation times T_2^{eff} at other resonance offsets, it must be recognized that the induction decays $G_x(t)$ and $G_y(t)$ as detected for large $\Delta\omega$ strongly oscillate. Therefore, it is advisable to consider the quantity $G(t) = \sqrt{G_x^2(t)/2 + G_y^2(t)/2}$ in the further analysis.

If it is assumed that the $G_\alpha(t)$ exhibit Gaussian shapes,[1] then the second moment of $G(t)$ to a very good approximation is given by $M_2 = (M_{2,x} + M_{2,y})/2$. The second moments due to the action of H_{D} are evaluated as usual via $M_{2,\alpha} = \mathrm{Tr}\{[\overline{H_{\mathrm{D}}}, I_\alpha]^2\}/\mathrm{Tr}\{I_\alpha^2\}$ with $\alpha = x, y$. A straightforward but tedious calculation shows that

$$M_{2,x} = M_2(0)\tilde{M}_{2,x}$$
$$\tilde{M}_{2,x} = (B_{zz} - B_{yy})^2 + B_{xy}^2 + B_{xz}^2 + 4B_{yz}^2. \qquad [13]$$

$M_{2,y}$ reads similarly but with all indices x and y appearing in Eq. [13] interchanged. The prefactor is the rigid lattice value of the second moment (*14*),

$$M_2(0) = 3I(I+1)\sum_{i\neq j}^{N} b_{ij}^2/N. \qquad [14]$$

For both pulse sequences, the maximum second moment, corresponding to a minimum relaxation time of the transverse magnetization T_2^{eff}, is given by $M_2^{\mathrm{max}} = \frac{5}{18}M_2(0)$.

In order to make explicit comparisons with experimental results it is convenient to introduce a full linewidth at half-maximum $\delta = \sqrt{2(\ln 2)\, M_2}$ which reads

$$\delta_{\mathrm{eff}} = \delta_{\mathrm{res}} + \delta_0\sqrt{\tilde{M}_{2,x} + \tilde{M}_{2,y}} \qquad [15]$$

[1] The assumption of a Gaussian shape is not crucial since analogous calculations with Lorentzian profiles yielded very similar results. The determination of the exact lineshapes is beyond the scope of this paper.

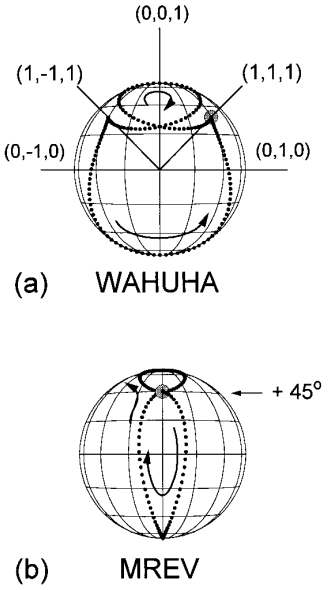

FIG. 3. Dots represent projections of the effective-field directions onto the surface of a unit sphere. Adjacent dots correspond to a change of 2° in the scaled resonance offsets $\tau_0\Delta\omega$. The $\mathbf{B}_{\text{eff}}$ axes change upon increasing the resonance offsets (from $\Delta\omega = 0$ as indicated by the circles) along the directions indicated by the arrows. Thereby they form a symmetric pattern on the anterior half of the sphere surface. Several thick lines are added to part (a) in order to define and show several coordinate and effective-field axes (x, y, z). Note that the x axis is normal to the plane of the paper and that adjacent intersections of two great circles correspond to a change of the polar (or the azimuthal) angle of 22.5°. The polar angle of 45° associated with the (1, 0, 1) direction is marked in (b).

when the residual linewidth δ_{res} is included. Note that various numerical constants have been lumped into the coefficient δ_0.

In order to treat the chemical-shift interactions, we note that isochromats evolving with a frequency $(\Delta\omega + \sigma)$, e.g., in a simple free-induction decay, will evolve with a reduced frequency $\Delta\omega_{\text{eff}} + \sigma_{\text{eff}} = S(\Delta\omega + \sigma)$ when detected stroboscopically under irradiation with one of the multiple-pulse sequences studied here. S is known as the chemical-shift scaling factor since it describes how much chemical-shift differences are apparently scaled down. To determine S, we must find out how the chemical-shift Hamiltonian $H_{\text{cs}} = -\sigma I_z$ (implicitly defined in Eq. [2]) transforms under large resonance offsets to yield an effective Hamiltonian

$$H_{\text{CS}}^{\text{eff}} = -\sigma \sum_{\alpha} C_\alpha I_\alpha. \qquad [16]$$

The coefficients C_α have a simple geometrical interpretation. They define the direction of the effective-field axes $\mathbf{B}_{\text{eff}}$. In Fig. 3, various effective-field directions are represented by their projections (shown as dots) onto the surface of a unit sphere. Adjacent dots correspond to incrementing the offset frequency by $(\pi/90\tau_0)$. The circles in this plot indicate that on resonance (or generally for $\tau_0\Delta\omega = n2\pi$) the effective field points along (1, 1, 1) for the WAHUHA sequence and along (1, 0, 1) for MREV. For increasing resonance offsets, the effective-field axes continuously change as indicated by the arrows. At $\tau_0\Delta\omega = (\pi/2)(+n2\pi)$, $\mathbf{B}_{\text{eff}}$ is oriented along (0, 0, 1) for the WAHUHA cycle while for MREV the effective field points into the $-z$ direction. For both sequences, these effective fields are simply inverted when the resonance offset has progressed by π further to $\tau_0\Delta\omega = (3\pi/2)(+n2\pi)$.

The scaling factor is then simply given by $S = \sqrt{\Sigma_\alpha C_\alpha^2}$. For the WAHUHA cycle, one has $S = \frac{1}{3}\sqrt{1 + \cos^2\tau_0\Delta\omega + \cos^4\tau_0\Delta\omega}$ while, for the MREV sequence, one finds

$$S = \tfrac{1}{3}\sqrt{1 + \cos^2\tau_0\Delta\omega + \cos^4\tau_0\Delta\omega - \cos^{10}\tau_0\Delta\omega}. \qquad [17]$$

It is interesting to note that in the latter case, for $\Delta\omega\tau_0$ slightly different from $n\pi$, the scaling factor is up to 3% larger than its conventional value of $S_0 = \sqrt{2}/3 = 0.471$ found at $\Delta\omega\tau_0 = n\pi$. For both cycles, the minimum scaling factor is $\frac{1}{3}$ at offset frequencies $\tau_0\Delta\omega = \pi/2 + n\pi$.

EXPERIMENTAL DETAILS

The NMR investigations were carried out in homebuilt spectrometers at a Larmor frequency of about 90 MHz. The 90° pulses were chosen to be 0.5–0.7 μs long. Since the flip angles of the RF pulses are in general not well defined, no measures were taken to achieve a particularly good RF homogeneity. All experiments were carried out at 233 K.

One set of experiments was performed in a homogeneous field under off-resonance conditions. The other set of experiments was conducted in a previously described static-gradient magnet (*5*) operated at gradient strengths of up to 111.5 T/m. In addition to the pulse cycles sketched in Fig. 1, we have used a cycle suggested by Müller and Scheler (*12*). This cycle is similar to the MREV sequence but with the following phases: $+Y-Y-Y-Y-Y+Y+Y+Y$. For our experiments we have used powders of *dl*-camphene obtained from Aldrich Co. at a nominal purity of 94%.

RESULTS AND DISCUSSION

Off-Resonance Experiments in Homogeneous Fields

For an understanding of the action of line-narrowing sequences in strong gradient fields, it is helpful to realize that in such a case the sample can be thought to be subdivided into thin slices of quasi-constant magnetic field. The variation of the Larmor frequency across the sample amounts to up to 1 MHz depending upon the experimental conditions given. Hence, it may be useful to conduct multiple-pulse experiments in homogeneous fields using various resonance offsets $\Delta\nu$ up to this magnitude. In order to mimic the

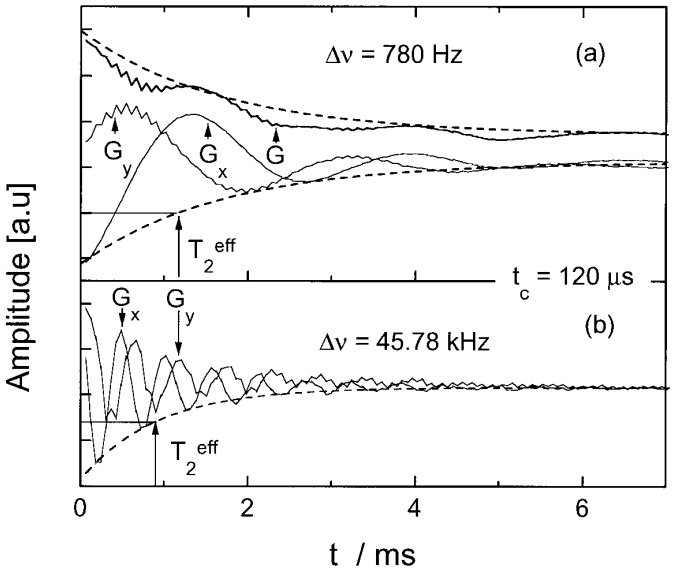

FIG. 4. Stroboscopically detected magnetizations G_x and G_y as they evolve under multiple-pulse irradiation. Here we have used the MREV sequence with $\tau_0 = 10$ μs for actual off-resonance frequencies (a) $\Delta\nu =$ 780 Hz and (b) $\Delta\nu = 45.78$ kHz. For (a) the experimental envelope $G = \sqrt{G_x^2 + G_y^2}$ (for clarity with offset) is also shown. The residual modulation of $G(t)$ is due to the imperfection of the quadrature detection since no phase cycling was performed. Note that for (b), aliasing leads to a seemingly smaller oscillation frequency of the signal. The dashed lines show the fit with an exponential decay function, whose characteristic decay time T_2^{off} is indicated by the arrows. The apparent off-resonance frequency $\Delta\nu_{\text{eff}}$ determined from the oscillation is always smaller than $\Delta\nu$.

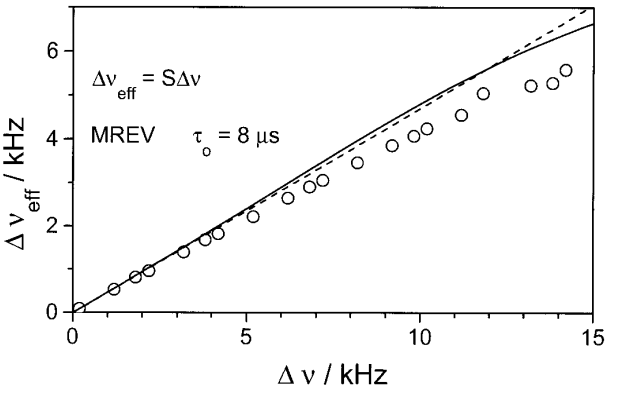

FIG. 5. Apparent resonance offset $\Delta\nu_{\text{eff}}$ vs the actual $\Delta\nu$ for the MREV sequence with $\tau_0 = 8$ μs. The scaling factor $S_0 = \sqrt{2}/3$ is represented by the dashed line. The solid line shows S calculated according to Eq. [17].

situation, the spectrometer adjustments (pulse lengths, phases, etc.) obtained on resonance were used for all $\Delta\nu$ in the experiments described in this section.

The efficiency of multiple-pulse sequences is demonstrated in Fig. 4 which shows the stroboscopically detected transverse magnetization components $G_x(t)$ and $G_y(t)$ recorded under MREV irradiation for two different resonance offsets. The magnetization decays were modulated with apparent resonance offsets $\Delta\nu_{\text{eff}}$. In Fig. 5 these offsets are plotted versus the actual $\Delta\nu$. For small $\Delta\nu$, a linear relationship $\Delta\nu = S\Delta\nu_{\text{eff}}$ with $S_0 = \sqrt{2}/3$ (dashed line) is obtained. For large $\Delta\nu$, the trend seen in the experimental data is sublinear, in qualitative agreement with the predictions of Eq. [17] (solid line). However, no quantitative agreement is achieved with this equation which was derived under several idealized conditions (δ-pulse approximation, use of truncated Hamiltonians, etc.). For still larger resonance offsets, no unambiguous determination of $\Delta\nu_{\text{eff}}$ is possible due to the fact that $G_\alpha(t)$ is detected stroboscopically. The envelope of the magnetization decay is conveniently obtained from $\sqrt{G_x^2(t) + G_y^2(t)}$ as shown in Fig. 4a. It is thus seen that the transverse magnetization dephases on time scales larger than 1 ms, which should be compared with the conventionally measured spin–spin relaxation time T_2 of about 70 μs.

The times at which the envelopes were decayed to half their initial values were read off from the traces (as indicated by the arrows in Fig. 4). The results were plotted only for positive resonance offsets $\Delta\nu < 500$ kHz in Fig. 6, since the pattern turned out to be symmetrical with respect to $\Delta\nu = 0$ (not shown). Figure 6a shows clearly that the MREV

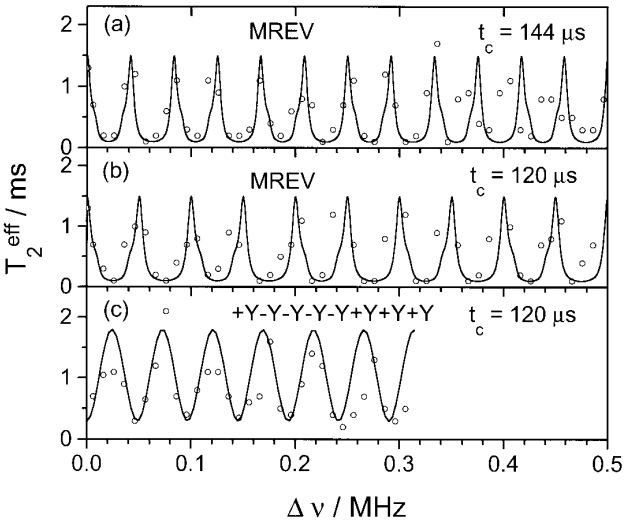

FIG. 6. Effective transverse dephasing times T_2^{eff} as a function of the actual off-resonance frequency $\Delta\nu$ measured in a homogeneous magnetic field. The labeling specifies the MREV and Müller–Scheler pulse sequences and the cycle times of $t_c = 120$ and 144 μs that were used in the different experiments. It is seen that a longer cycle time leads to an enhanced modulation of the $T_2(\Delta\nu)$ pattern consistent with $\Delta\nu = n/(2\tau_0)$. The solid lines in (a) and (b) were calculated using Eq. [15] with $1/\delta_0 = 46$ μs and $1/\delta_{\text{res}} =$ 1.5 ms adjusted to match the minimum and maximum effective relaxation times T_2^{eff}. Note that, while optimum line narrowing is achieved at frequencies $\Delta\nu = n/(2\tau_0)$ apart, the theoretical curves are periodic with frequency $\Delta\nu = n/\tau_0$. In (c) the use of the Müller–Scheler sequence (*12*) is seen to be very ineffective for zero offset because the entire pattern is simply ''phase'' shifted by (half) an oscillation period. The solid line in (c) is a guide to the eye.

sequence is not only particularly effective on resonance but also for $\Delta\nu = n/(2\tau_0)$ up to very large n. The inverse proportionality between $\Delta\nu$ and τ_0 is also evident from Fig. 6b where a shorter pulse spacing is seen to lead to a less rapid modulation of the $T_2(\Delta\nu)$ pattern. A shift of this pattern along the abscissa by $1/(2\tau_0)$ can be achieved by using the Müller–Scheler sequence, as demonstrated in Fig. 6c.

The modulation frequencies of these patterns and of those from experiments using the WAHUHA sequence (not shown) obtained for pulse spacings 6 μs $\leqslant \tau_0 \leqslant$ 12 μs all were in good agreement with Eq. [12].

The solid lines in Figs. 6a and 6b were calculated from $T_2^{\text{eff}} = 1/\delta_{\text{eff}}$ with δ_{eff} given by Eq. [15]. Agreement with the experimental data is good except at the largest $\Delta\nu$. These deviations could be ascribed to the finite pulse lengths and the nonideal flip angles which are most pronounced at large $\Delta\nu$. These effects were not explicitly taken into account in our calculations.

Experiments in Large Static-Field Gradients

In order to demonstrate the performance of the line-narrowing sequences in static gradient fields, we have first conducted a Hahn-echo experiment with three cycles of an MREV sequence with $\tau_0 = 14$ μs inserted in the dephasing and the rephasing periods (cf. inset of Fig. 7). The spectrum obtained from the magnetization recorded after 2τ is shown in Fig. 7b. Its envelope $B(\Delta\nu)$ is bell-shaped as is the Fourier transform of a conventional Hahn echo, also shown in Fig. 7a. The width of $B(\Delta\nu)$ is due to the finite excitation widths of the RF pulses, in combination with the limited bandwidth of our resonance circuit. More interesting is the fine structure observed in the spectrum. At least at small offsets $|\Delta\nu| < 300$ kHz, maxima appear with an average separation in frequency of about $\nu_{\text{mod}} = 1/(2\tau_0) = 36$ kHz. This is clearly seen in Fig. 7c, where we also plot the function $I(\Delta\nu) = B(\Delta\nu)[\sin(2\pi\Delta\nu/\nu_{\text{mod}}) + A]$. Here A is an empirical coefficient accounting for the difference in intensity between the local maxima and minima of the spectrum. From Fig. 7c it is clearly seen that every second minimum is considerably lower than accounted for by the empirical function. The existence of this low-frequency component in the spectrum can be rationalized by noting that while the maximum line narrowing is achieved for every $\Delta\omega = n\pi/\tau_0$, the line-narrowing effect of the MREV sequence is only periodic with respect to $2\pi/\tau_0$.

In the following we will briefly discuss some implications for the study of solid-state diffusion using large magnetic-field gradients g in modified stimulated-echo experiments (*9*). First of all it should be noted that the difference in dephasing and rephasing frequencies of tagged nuclei are reduced by the scaling factor S. Although this coefficient depends quite strongly on $\Delta\nu$, only those slices within the sample will contribute significantly to the stimulated echo

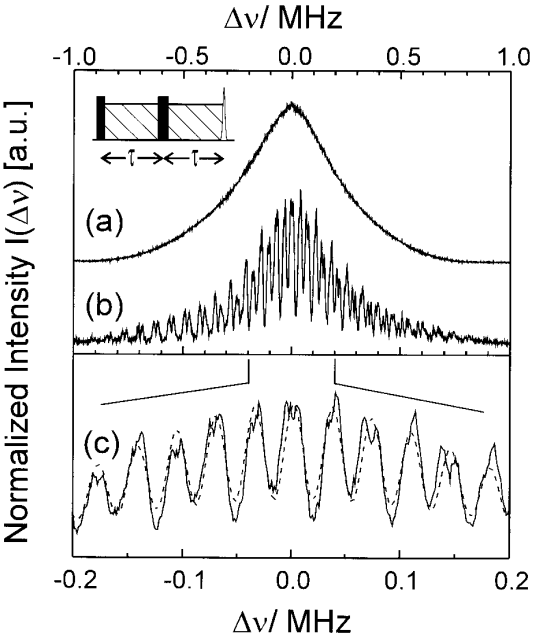

FIG. 7. (a) Spectrum of the excitation profile measured using the Fourier transform of the Hahn echo as sketched in the inset with no RF irradiation during the shaded intervals. The evolution times τ were set to 50 μs. The shape of the spectrum is approximately Gaussian with a width of about 1 MHz. The finite width is due to the combined effect of the finite pulse length (0.5 μs for a 90° pulse) and the limited bandwidth of our resonance circuit. (b) Spectrum measured with a Hahn echo employing MREV irradiation (with $\tau_0 = 14$ μs) during the shaded intervals. Here τ was 504 μs and contained three MREV cycles. It is seen that, for a number of frequencies satisfying the condition $\Delta\nu = n/2\tau_0$, the multiple-pulse irradiation leads to a considerable enhancement of the spectral intensity. Note that the curves shown as (a) and (b) are not drawn to scale, but have been normalized to the same height. (c) Enlarged presentation of the central portion of the spectrum shown in (b). The dashed line is calculated using $I(\Delta\nu) = B(\Delta\nu)[\sin(2\pi\Delta\nu/\nu_{\text{mod}}) + A]$; see text.

for which Eq. [12] is fulfilled. Hence, the relevant scaling factor will in general be only very slightly different from its low-offset value S_0 and consequently the effective gradient to a very good approximation is given by $g_{\text{eff}} = S_0 g$.

The maximum scaling factor of the eight-pulse sequence is smaller by a factor of about 1.2 than that of the four-pulse cycle. Therefore, the latter should be slightly superior for the determination of very small diffusion coefficients. The larger robustness of the MREV cycle against various pulse imperfections (*13*) which are unavoidable in magnetic-field-gradient experiments, however, is expected to outweigh this potential advantage.

CONCLUSIONS

In order to document the action of line-narrowing sequences in large static-magnetic-field gradients which were previously used in NMR diffusion studies, we have investigated the far-off-resonance performance of the WAHUHA

and MREV multiple-pulse cycles. By increasing the resonance offsets beyond about 15 kHz, in accord with previous studies, we find that the line-narrowing efficiency of multiple-pulse irradiation rapidly deteriorates. But upon further increasing $\Delta\nu$, the effective transverse relaxation times $T_2^{\text{eff}}(\Delta\nu)$ pass through a minimum and later reach values as long as those determined near resonance. The modulation frequency of this $T_2^{\text{eff}}(\Delta\nu)$ pattern depends strongly on the basic pulse separation τ_0 in the multiple-pulse cycles and repeats itself several times up to about $\Delta\nu = 300$ kHz. This means that, up to this large frequency offset, efficient line narrowing was demonstrated in our experiments. The slightly degraded performance seen at the largest offsets is due to several technical limitations. In our case these are given by the relatively narrow bandwidth of the resonance circuit and to a lesser extent by the finite pulse widths.

From our theoretical considerations, it became clear that in the general case the conventionally employed average Hamiltonian theory is not applicable. Therefore, we have separated the transformed dipolar interaction, which was treated in the short-time approximation, from the off-resonance and the chemical-shift terms which could be fully evaluated analytically. Efficient line narrowing was predicted to occur at resonance offsets $\Delta\omega = n\pi/\tau_0$, as confirmed by experiments in static-field gradients as well as in homogeneous fields.

Thus contrary to what one may have expected initially, it is not only the magnetization from a single thin slice near $\Delta\nu = 0$ which contributes to the measured signal in studying solid-state diffusion with the MREV sequence in static magnetic fields. We have shown that an efficient prolongation of the effective spin–spin relaxation times can be achieved for a large number of slices distributed over the entire excited sample volume. It is of course this prerequisite which ensures a sufficient signal-to-noise ratio and facilitates diffusion studies to be carried out in an acceptable measuring time.

ACKNOWLEDGMENTS

We thank U. Haeberlen for bringing Ref. (*12*) to our attention. Funding by the Deutsche Forschungsgemeinschaft (SFB262/D9) is gratefully acknowledged.

REFERENCES

1. D. C. Ailion, *Adv. Magn. Res.* **5,** 177 (1971).
2. D. C. Ailion and J. A. Norcross, *Phys. Rev. Lett.* **74,** 2383 (1995); G. Papvassiliou, A. Leventis, F. Milia, and J. Dolinsek, *Phys. Rev. Lett.* **74,** 2387 (1995).
3. G. Fleischer and F. Fujara, ''NMR Basic Principles and Progress,'' Vol. 30, p. 159, Springer-Verlag, Berlin, 1994.
4. P. T. Callaghan, ''Principles of Nuclear Magnetic Resonance Microscopy,'' Clarendon Press, Oxford, 1991.
5. I. Chang, F. Fujara, B. Geil, G. Hinze, H. Sillescu, and A. Tölle, *J. Non-Cryst. Solids* **172–174,** 674 (1994).
6. P. T. Callaghan and J. Stepisnik, *Phys. Rev. Lett.* **75,** 4532 (1995).
7. J. S. Waugh, L. M. Huber, and U. Haeberlen, *Phys. Rev. Lett.* **20,** 180 (1968).
8. W.-K. Rhim, D. D. Elleman, and R. W. Vaughan, *J. Chem. Phys.* **58,** 1772 (1973).
9. I. Chang, G. Hinze, G. Diezemann, F. Fujara, and H. Sillescu, *Phys. Rev. Lett.* **76,** 2523 (1996).
10. U. Haeberlen, J. D. Ellett, Jr., and J. S. Waugh, *J. Chem. Phys.* **55,** 53 (1971); W.-K. Rhim, D. D. Elleman, and R. W. Vaughan, *J. Chem. Phys.* **59,** 3740 (1973).
11. W.-K. Rhim, D. D. Elleman, L. B. Schreiber, and R. W. Vaughan, *J. Chem. Phys.* **60,** 4595 (1974).
12. R. Müller and G. Scheler, *Ann. Phys.* **36,** 304 (1979).
13. U. Haeberlen, ''High Resolution NMR in Solids, Selective Averaging,'' Academic Press, New York, 1976.
14. M. Goldman, ''Spin Temperature and Nuclear Magnetic Resonance in Solids,'' Clarendon Press, Oxford, 1970.